# EVALUATION OF FIRE ENGINEERING DESIGN CORRELATIONS FOR EXTERNALLY VENTING FLAMES USING A MEDIUM-SCALE COMPARTMENT-FAÇADE FIRE EXPERIMENT

**E. K. Asimakopoulou*, D. I. Kolaitis* and M. A. Founti***
elasimak@mail.ntua.gr
* Laboratory of Heterogeneous Mixtures and Combustion Systems, Thermal Engineering Section,
School of Mechanical Engineering, National Technical University of Athens,
9 Heroon Polytechneiou St., Polytechneioupoli Zografou, Athens 15780, Greece.

## Abstract
In a fully developed under-ventilated compartment fire, flames may spill out of external openings (e.g. windows); Externally Venting Flames (EVF) pose a significant risk of fire spreading to adjacent floors or buildings. The main scope of this work is to comparatively assess a range of fire engineering design correlations used to describe the external dimensions of the EVF envelope. The predictive accuracy of each correlation is evaluated through comparison with experimental data obtained in a medium-scale compartment-façade fire arrangement, using a variety of fire load levels. A series of medium-scale fire compartment experiments is performed, employing a ¼ scale model of the ISO 9705 room equipped with an extended façade. An extensive sensor network is used aiming to monitor the dynamic behaviour of a broad range of important physical parameters (e.g. gas and surface temperatures, heat flux, fuel mass loss, gas concentrations). A dedicated image processing tool is developed to allow estimation of the EVF envelope main dimensions (e.g. height, width, projection). An "expendable" fuel source (n-hexane liquid pool fire) is utilized to effectively simulate realistic building fire conditions. Digital camera imaging is used to determine the main geometrical characteristics of the EVF envelope. Comparison of fire engineering design correlation predictions with experimental data reveals that correlations for the estimation of EVF height err on the safe side in under-ventilated fire conditions; increasing the heat release rate results in more conservative EVF height and projection predictions. It is shown that EVF projection and width strongly depend on both excess heat release rate and height. In addition, the necessity to derive appropriate criteria for the identification of the EVF projection is demonstrated. The obtained extensive set of experimental data can be used to validate CFD models or evaluate the accuracy of other available fire design correlations.

## 1. INTRODUCTION
In a fully developed under-ventilated compartment fire, flames may spill out of external openings (e.g. windows), should the glazing fail. Externally Venting Flames (EVF) pose a significant risk of fire spreading to adjacent floors or buildings; this risk is constantly increasing due to the rising use of combustible insulation materials in building façades [1]. However, the majority of current fire safety codes are lacking accurate methodologies to evaluate the risks associated with EVF, especially in an ever-changing environment where new façade design requirements and construction materials challenge the established fire safety solutions.
In order to effectively act towards EVF prevention and mitigation of external fire spread, it is essential to investigate the fundamental physical phenomena associated with EVF. Research

on EVF, focused on identifying the main physical parameters governing internal fire dynamics and consequent EVF, commenced in the early 1960's by Yokoi [2] and was further expanded by others [3-5]. Some findings of the respective research regarding EVF description and its impact on façades have been gradually incorporated in fire safety codes and design guidelines. The Eurocode design guidelines [6], currently implemented in the E.U., provide general principles and rules regarding thermal and mechanical actions on structures exposed to fire; fire actions for designing load-bearing structures are prescribed in EN 1991 (Eurocode 1) [6]. However, fire spreading due to combustible façade materials is not addressed at all in the Eurocode guidelines and there is only a coincidental reference to risks associated with EVF (i.e. protection of steel and timber building elements).

This work is motivated by an increasing number of recent reports [7-11] suggesting that existing engineering design methodologies cannot describe with sufficient accuracy the characteristics of EVF under realistic fire load conditions. The main scope of this work is to comparatively assess fire engineering design correlations used to describe the external dimensions of the EVF envelope [5,6,12]. The predictive accuracy of each correlation is evaluated through comparison with experimental data obtained in a medium scale compartment-façade fire arrangement, using a variety of fire load levels.

## 2. FIRE ENGINEERING DESIGN CORRELATIONS RELATED TO EVF

There are several fire engineering design correlations available [2-4,7,8,11,], aiming to describe the main characteristics of EVF that may affect the fire safety design aspects of a building, such as the EVF's height, projection, temperature and heat flux to the façade. These semi-empirical correlations have been derived using simplified theoretical analyses in conjunction with experimental data [2, 13]. Although EVF exhibit significantly different characteristics depending on the number and position of openings in the fire compartment, in the current study only fire compartments with a single opening are investigated.

Estimation of EVF dimensions and main thermal characteristics is commonly based on using the conservation laws of mass, momentum and energy for upward gas flows [2,10,14]. The geometrical characteristics of the EVF envelope are known [6, 14] to generally be affected by fire heat release rate ($Q$), average height of the opening(s) ($h_{eq}$), total area of the opening(s) ($A_v$) and external wind speed ($V$). Even though the geometrical boundaries of the EVF envelope are dynamically changing with time, fire engineering correlations commonly assume a steady-state EVF shape, prescribed via EVF height ($L_L$), projection ($L_H$) and width ($w_f$) (Figure 1). EVF is commonly considered to project from the upper part of the opening, initially at an angle but, due to thermal buoyancy effects, the fire plume eventually advances vertically, parallel to the façade wall (Figure 1).

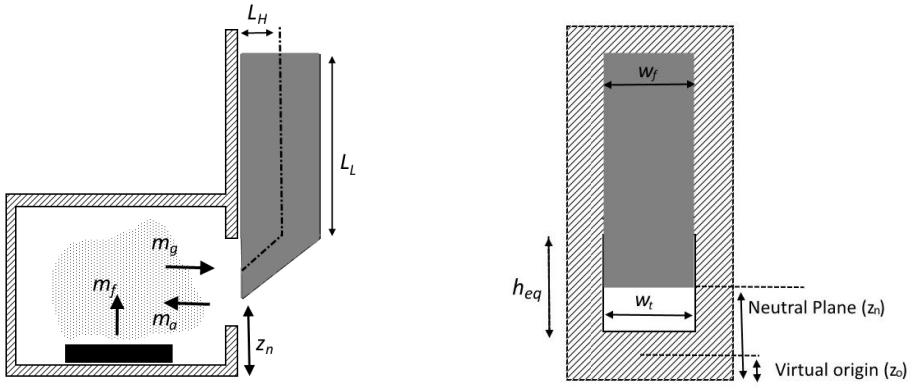


**Figure 1.** General schematic illustrating the main characteristics of EVF.

A range of semi-empirical correlations used to estimate EVF height ($L_L$) and projection ($L_H$) is presented in Table 1 [2,5,6,12,13,15-17]. In general, the EVF height is considered to be proportional to the fire heat release rate ($Q$) or excess heat release rate ($Q_{ex}$) and inversely proportional to the "effective" diameter of the fire source ($D_v$). The latter quantity represents the area of the opening through which the EVF is ejected and can be estimated using Equation (1) [3,5].

$$D_v = w_t\,(h_{eq}/2) \tag{1}$$

$$Q_{ex} = Q - Q_{ins,m} = Q - 1500 D_v (h_{eq})^{1/2} \tag{2}$$

The excess heat release rate ($Q_{ex}$) corresponds to the fraction of the total heat release rate that is owed to combustion that takes place out of the fire compartment (EVF). Recently [5], a correlation to estimate $Q_{ex}$ for under-ventilated conditions has been proposed (Equation 2); in this case, the total heat release rate ($Q$) is assumed to be the sum of the average heat release rate at the interior of the fire compartment ($Q_{ins,m}$) and the excess heat release rate ($Q_{ex}$) at the exterior of the fire compartment.

**Table 1**: Semi-empirical correlations for EVF height ($L_L$) and projection ($L_H$).

| **Abbr.** | **Ref.** | $\boldsymbol{L_L}$ (m) |
|---|---|---|
| H1 | [6] | $h_{eq}\left[2.37\left(\frac{Q}{A_v\rho_\infty\left(h_{eq}\right)^{1/2}}\right)^{2/3}-1\right]$ |
| H2 | [12] | $D_v\,[-1.02 + 0.23(Q^{2/5}/D_v)]$ |
| H3 | [5] | $z_n + 2l\left(\frac{Q_{ex}}{\rho_\infty c_p T_\infty g^{1/2} l^{5/2}}\right)^{0.44}$ |
| **Abbr.** | **Ref.** | $\boldsymbol{L_H}$ (m) |
| P1 | [6] | $\begin{cases} h_{eq}/3 & , h_{eq} \le 1.25 w_t \\ 0.3 h_{eq}(h_{eq}/w_t)^{0.54} & , h_{eq} > 1.25 w_t \text{ and } w_d > 4 w_t \\ 0.454 h_{eq}(h_{eq}/2w_t)^{0.54} & , h_{eq} > 1.25 w_t \text{ and } w_d < 4 w_t \end{cases}$ |
| P2 | [2] | $0.13 \cdot L_L$ |
| P3 | [16] | $0.195 \cdot L_L$ |
| P4 | [17] | $0.119 \cdot L_L$ |

Correlation H1 and P1, employed in Eurocode 1 [6], are based on the correlations proposed by Law [13]. Assuming an axisymmetric buoyant plume, correlation H2 [12] uses the "effective" diameter of the fire source and heat release rate to estimate the mean EVF height. A modified model for the estimation of EVF height, expressed via correlation H3, was recently proposed [5]; the characteristic length scale $l$ is calculated using Equation (3). Correlations P2 [2], P3 [16] and P4 [17], used to estimate the EVF projection, are based on flow analysis methodologies assuming non radiative heat sources located at the upper half of the opening.

$$l = w_t\, h_{eq} (h_{eq})^{1/2} \tag{3}$$

Although some [2,12,16,17] of the correlations are derived from open air pool fire experimental data, they can be also used for the determination of EVF average dimensions by assuming the upper half of the opening as the fuel source [14]. In such a case, only the convecting fraction of the heat release rate at the opening is taken into account since the compartment size does not have a notable influence on the EVF geometrical characteristics [19].

The EVF width ($w_f$) is commonly assumed to be equal to the opening width ($w_t$) [6,13]; only scarce reports in the literature [18] indicate its dependence on EVF height and aspect ratio of the opening ($w_t/h_{eq}$). It has been observed that when the fire load burns unevenly, it may result in asymmetric EVF projection and width [13]; such behaviour is not taken into account in any of the correlations currently available. In all cases, the external dimensions of an EVF are assumed constant in time (steady-state conditions) enabling estimation of the geometrical properties using simple trigonometry rules [6,10,13].

## 3. EXPERIMENTAL SETUP

### 3.1 Medium-Scale Compartment-Façade Fire Apparatus

A series of fire experiments were conducted in a medium-scale compartment-façade fire apparatus. The compartment was a ¼ scale model of an ISO 9705 room [20]. The internal compartment dimensions were 0.60 m x 0.90 m x 0.60 m; the external facade wall measured 0.658 m x 1.8 m. A double layer of 0.0125 m thick fireproof gypsum plasterboards was used as an internal and external lining material. The fire compartment opening, located in the middle of the north wall, measured 0.20 m x 0.50 m. A schematic of the experimental apparatus, illustrating the locations of the utilized measuring devices, is given in Figure 2.

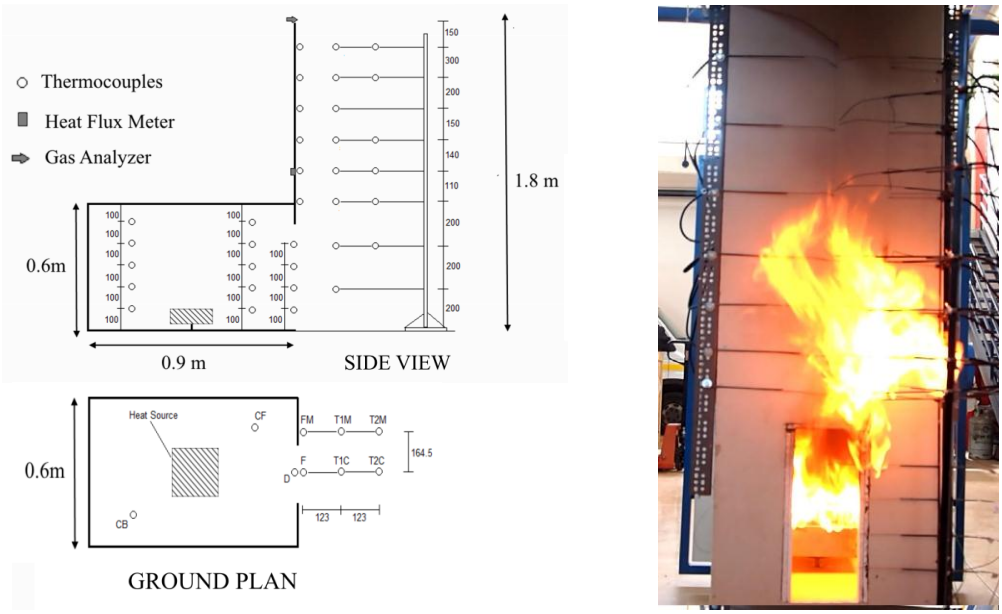


**Figure 2.** General layout (left) and a characteristic photograph (right) of the medium-scale compartment-façade fire apparatus.

### 3.2 Parametric Study: Fire Load

Gaseous burners are commonly used in relevant fire compartment experiments [4,5,18], to provide a constant (steady-state conditions) fire source. However, aiming to achieve more "realistic" fire conditions, relevant to actual building fires, an "expendable" (transient conditions) fuel source was used. A stainless steel rectangular pan, measuring 0.25 m x 0.25 m x 0.10 m, was located in the geometrical centre of the compartment's floor; n-hexane was

used as the liquid fuel of choice. The mass of the fuel source, n-hexane was continuously monitored via a load cell, installed under the pan. The fuel pan size was selected in order to achieve under-ventilated fire conditions, thus forcing the flames to eject through the opening. A series of experiments were conducted modifying the total fuel load; a summary of the main operational parameters, such as ambient temperature ($T_\infty$) and relative humidity ($RH_\infty$), total fire duration ($t_{dur}$), fuel mass ($m_f$), global equivalence ratio (GER) [24], total heat release rate ($Q$), average heat release rate in the interior of the fire compartment ($Q_{ins,m}$) and excess heat release rate ($Q_{ex}$) [5], of the 3 test cases examined, is shown in Table 2. Test cases 2 and 3 corresponded to under-ventilated fire conditions; in test case 1, a slightly over-ventilated fire was developed, due to low fire load used.

**Table 2.** Summary of main operational parameters for the examined test cases.

| **Test Case** | $T_\infty$ ($^o$C) | $RH_\infty$ (%) | $t_{dur}$ (s) | $m_F$ (kg) | $GER$ (-) | $Q$ (kW) | $Q_{ins,m}$ (kW) | $Q_{ex}$ (kW) |
|---|---|---|---|---|---|---|---|---|
| 1 | 25.8 | 42.0 | 372 | 0.655 | 0.735 | 79 | - | - |
| 2 | 26.7 | 42.0 | 525 | 1.539 | 1.224 | 132 | 106.5 | 25.5 |
| 3 | 26.5 | 47.0 | 595 | 6.078 | 2.159 | 233 | 106.5 | 126.5 |

### 3.3 Measuring Devices: Developing Thermal-Field

The overall thermal behaviour of the compartment-façade configuration was investigated by measuring temperatures and heat fluxes at various locations. 10 K-type 1.5 mm diameter thermocouples, located in the front and rear corner of the compartment and 4 thermocouples vertically distributed in the centreline of the opening were used to monitor the temperature profiles developing at the interior of the fire compartment. Emphasis was given to the characterization of the temperature environment adjacent to the façade wall along the height of the fire plume both in the centreline and off-axis positions (164.5 mm from the centreline). Towards this end, 14 thermocouples were placed in various locations across the façade wall, whereas 27 additional thermocouples were distributed among two thermocouple trees, located at a distance of 123 mm and 246 mm from the façade wall, respectively (Figure 2). A water-cooled, 25 mm diameter, Schmidt-Boelter heat flux sensor was placed at the centreline of the façade surface facing the EVF, 0.11 m above the opening. All thermocouples and heat flux measurements were recorded using a Universal Data Logging Interface designed in LabView software; the sampling frequency was 1 s. A thermal camera was positioned 6.0 m away from the apparatus facing the façade to record additional information regarding the thermal response of the façade surface.

### 3.4 Measuring Devices: EVF Envelope Dimensions

Two digital video cameras were positioned at two locations, opposite and at a right angle to the opening, recording the developing EVF envelope, at 30 frames per second. Time series of video frames were obtained and processed using an in-house developed MATLAB code, aiming to determine the geometric characteristics of the EVF envelope. Each image frame was cropped, aligned and assigned proper world coordinates. A modified version of the methodologies proposed by Vipin and Celik et al. [21,22] was used. Each frame was converted into a binary image using a set of rules, employing appropriate threshold limits for Red, Green and Blue colour levels and luminosity, based on the prevailing lighting conditions in each test case. The threshold limits were acquired through an extended statistical analysis of the various flame regions in each stage of the flame cycle. The EVF envelope dimensions were determined by calculating the average flame probability (intermittency). Early research

[16] indicated that the fire plume above a fuel source can be divided into three main regions, characterised by the probability of flame presence. Using flame intermittency criteria, these three distinct regions, namely the "continuous flame", the "intermittent flame" and the "far-field plume", can be also identified in EVF [5,28]. In this context, the flame height corresponding to the "continuous flame" ($L_{f\_0.95}$, 95% intermittency), "intermittent flame" ($L_{f\_0.50}$, 50% intermittency) and "far-field plume" ($L_{f\_0.05}$, 5% intermittency) regions was obtained; beyond these regions the flame cannot be seen and only hot combustion products are present. The mean EVF height ($L_{f,m}$) can be estimated using either the 50% flame intermittency limit ($L_{f\_0.50}$), or, alternatively, by averaging the estimated flame height at the "continuous flame" ($L_{f\_0.05}$) and "far-field plume" ($L_{f\_0.95}$) regions [23]; values obtained using both methodologies are in very good agreement.

## 4. RESULTS AND DISCUSSION

### 4.1 Fuel Consumption Rate

The combustion rate of pool fires in compartments is influenced by a variety of parameters, such as ventilation, radiation from the surrounding walls and thermal characteristics of the exposed rim above the fuel [3,24]. The effects of these parameters are evident in Figure 3, where measurements of the instantaneous fuel mass consumption rate for all the examined test cases are depicted. It is evident that higher initial fuel mass results in enhanced fuel combustion rates. In addition, as time advances, the gradual lowering of the liquid fuel level results in a slight increase of the instantaneous fuel combustion rate.

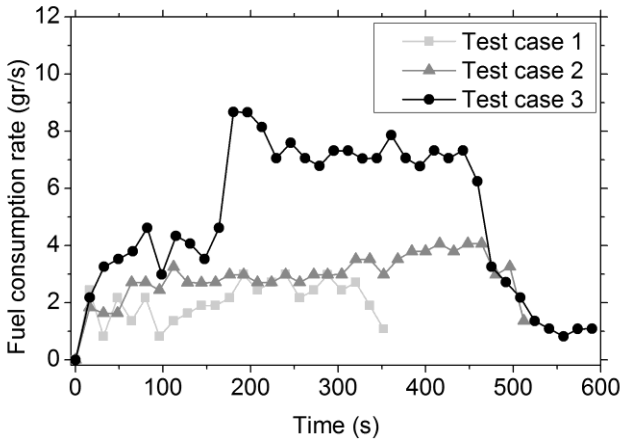


**Figure 3.** Measurements of instantaneous fuel mass consumption rate.

### 4.2 Compartment Gas Temperatures

Gas temperature evolution inside the compartment exhibits similar characteristics for each test case; the three stages of fire growth, quasi-steady state (corresponding to fully developed fire conditions) and decay phase, typically encountered in compartment fires, can be easily identified (Figure 4). As expected, higher fire loads result in higher gas temperatures. The vertical distribution of the gas temperature at the front of the compartment, near the opening (location CF), is notably higher in Test case 3, indicating that combustion still occurs further away from the fuel pan, resulting in a larger EVF ejecting from the opening (c.f. Figure 6).

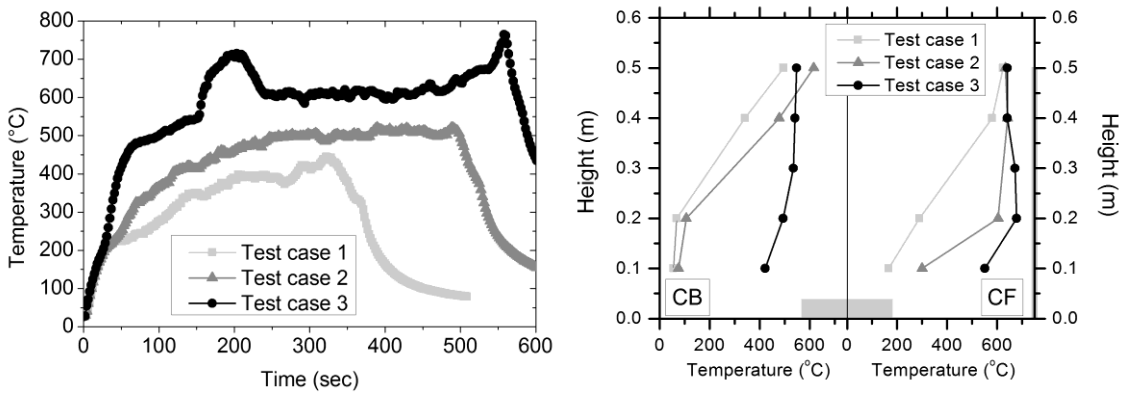


**Figure 4.** Temporal variation of upper gas layer temperature (left) and vertical distribution of time-averaged air temperature (right) at the interior of the fire compartment.

### 4.3 EVF Gas Temperatures

Figure 5 depicts the vertical distribution of time-averaged values for the maximum and mean air temperature of EVF, at a distance of 123 mm (T1C) and 246 mm (T2C) away from the façade. All measurement locations correspond to the EVF envelope, covering both the "continuous flame" and the "intermittent flame" regions. Temperatures at the "continuous flame" region remain practically constant; a slight temperature decrease is observed throughout and above the "intermittent flame" zone. In Test case 3, significantly higher EVF temperatures are observed, compared to Test cases 1 and 2.

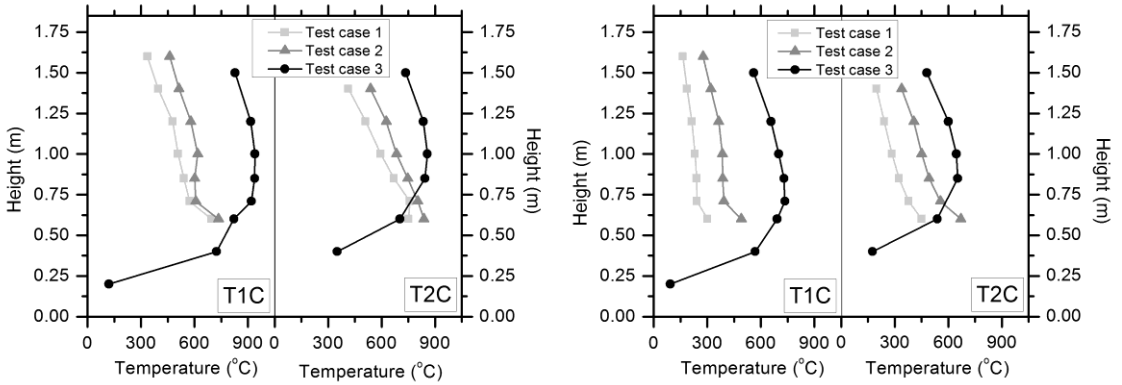


**Figure 5.** Vertical distribution of time-averaged maximum (left) and mean (right) EVF temperatures, at a distance of 123 mm (T1C) and 246 mm (T2C) from the façade.

### 4.4 EVF Envelope Dimensions

The calculated spatial distribution of flame envelope probability, expressed via the flame intermittency, is illustrated in Figure 6 (image artifacts are owed to the presence of the thermocouple trees). The overall EVF volume generally increases with increasing heat release rate. The EVF shape in low fire load and over-ventilated fire conditions (Test case 1), is significantly limited in comparison to higher fire load under-ventilated fire conditions (Test cases 2 and 3). In general, the EVF envelope tends to assume an elliptical shape, which is compatible to the EVF shapes proposed in widely used engineering design methodologies [2,10].

Flame ejection through the opening occurs due to ignition of the excess (unburnt) fuel and expansion of the buoyant turbulent flame at the exterior of the compartment. Whether an EVF would develop mainly depends on the fuel concentration and the temperature of the hot unburnt gases exiting the fire compartment. A summary of estimated values for the EVF

height at the continuous ($L_{f\_0.95}$), intermittent ($L_{f\_0.50}$) and far field ($L_{f\_0.05}$) regions, mean EVF height ($L_{f,m}$), mean width ($w_f$) and projection ($L_H$) is presented in Table 3. The EVF probability ($P$) corresponds to the fraction of the total fire duration that EVF emerges at the exterior of the fire compartment; $P$ is strongly affected by the overall heat release rate, an observation that agrees with similar remarks found in the literature [26].

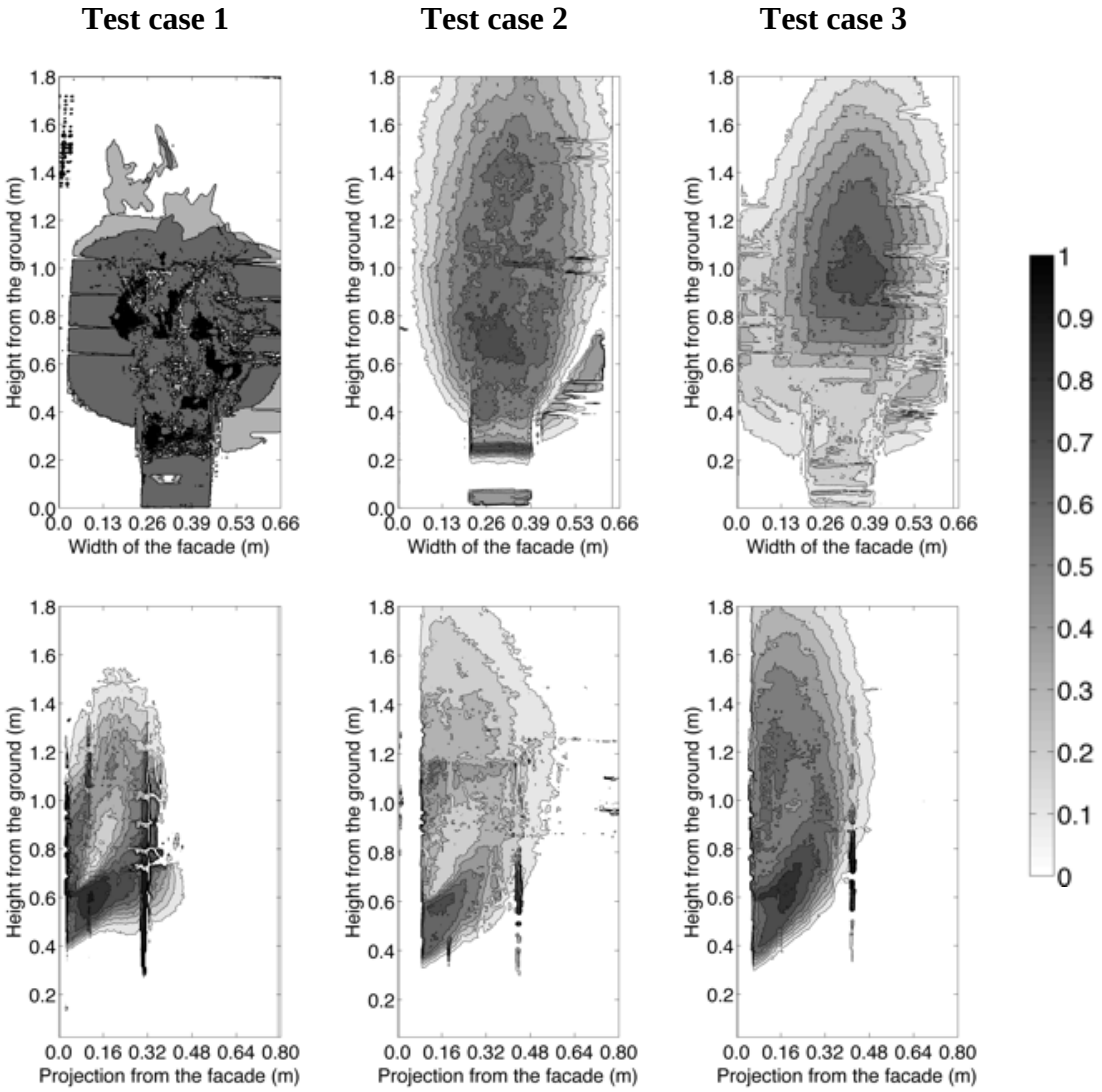


**Figure 6.** Front (top) and side (bottom) views of flame intermittency contours.

**Table 3.** Summary of experimentally determined values of EVF height, width and projection.

| Test case | Test duration | EVF duration | $L_{f\_0.05}$ | $L_{f\_0.50}$ | $L_{f\_0.95}$ | $L_{f,m}$ | $w_f$ | $L_H$ | $P$ |
|---|---|---|---|---|---|---|---|---|---|
| | | | (m) | | | | | | |
| 1 | 372 | 172 | 1.37 | 1.026 | 0.51 | 0.94 | 0.4268 | 0.229 | 0.6143 |
| 2 | 525 | 288 | 1.79 | 1.278 | 0.62 | 1.205 | 0.4310 | 0.348 | 0.8090 |
| 3 | 595 | 541 | 1.77 | 1.354 | 0.879 | 1.3245 | 0.4046 | 0.335 | 0.9344 |

Figure 7 illustrates the methodology followed to estimate the mean flame height, $L_{f\_0.50}$. The variation of time-averaged flame intermittency with height, at the centreline of the flame, is depicted; flame intermittency decreases with height from higher values (approaching unity) to smaller values (in the intermittent flame region) until zero values are reached. The mean

flame height is assumed to be equal to the largest height value where 50% flame intermittency is observed (marked with an asterisk in Figure 7). In Figure 7, EVF height predictions, using the semi-empirical correlations H1, H2 and H3 (presented in Table 1) are also depicted. Good levels of quantitative agreement are observed; fire engineering design correlations are found to err on the safe side when under-ventilated fire conditions are considered (Test cases 2 and 3), whereas in over-ventilated fire conditions a slight under-prediction is observed.

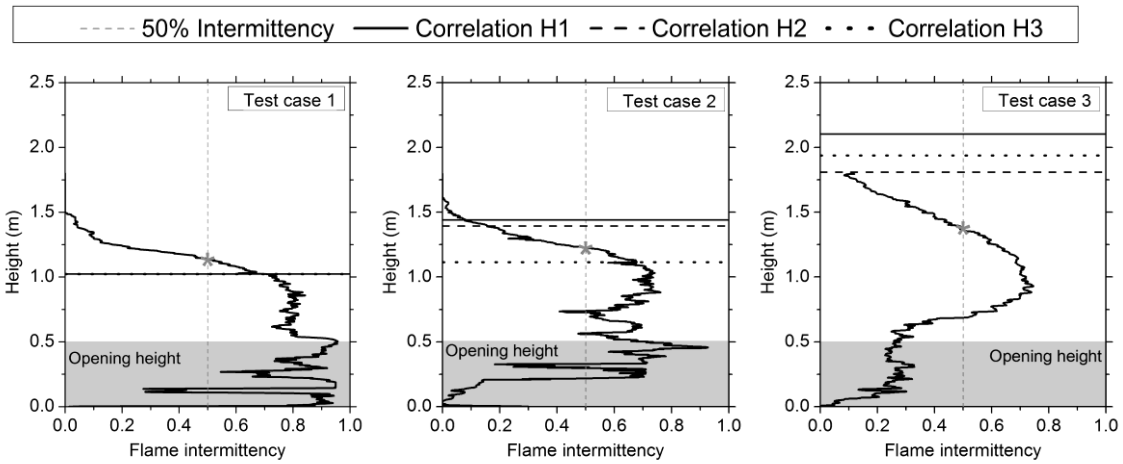


**Figure 7.** Determination of mean flame height using experimental data and empirical correlations.

The temporal evolution of the instantaneous EVF height, expressed via the $L_{f\_0.50}$ at the centreline, is illustrated in Figure 8; these values are estimated using the methodology presented in Figure 7 for all time frames captured in the cameras. A typical behaviour for an EVF developing in an under-ventilated compartment fire can be observed [27], which is characterized by 3 distinct phases that appear in succession. Initially, combustion is constrained in the interior of the fire compartment ("internal flaming") and in the vicinity of the fuel pan an advection stream is created. Gradually, the flame front moves away from the fuel pan, expanding radially and horizontally towards the opening. In that phase, external flame jets and quick flashes appear at the exterior of the fire compartment, signifying the beginning of the "intermittent flame ejection" stage. As time passes, "consistent external flaming" is observed due to the sustained external combustion of unburnt volatiles, during the quasi-steady phase of fully developed fire. Throughout the latter phase, EVF consistently covers the region above the opening resulting in higher values of EVF height.

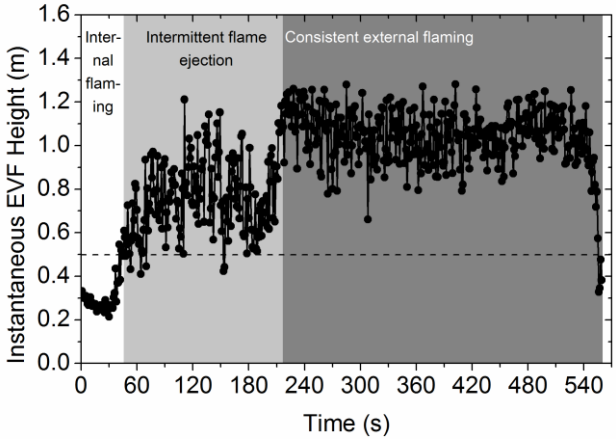


**Figure 8.** Temporal evolution of instantaneous flame height for Test case 3.

The EVF projection ($L_H$) was estimated using the time-averaged values of the flame intermittency at a height 0.9 m above the ground. Unlike to the calculation methodology used to evaluate $L_{f\_0.50}$, it is not a straightforward procedure to define the mean value of $L_H$, since the flame intermittency is not monotonically decreasing. In this case, $L_H$ was assumed to be equal to the largest distance from the façade where a 50% flame intermittency is observed (marked with an asterisk). Figure 9 depicts schematically the variation of flame intermittency as a function of the distance from the façade; estimated values for the EVF projection, using the semi-empirical correlations P1-P4 presented in Table 1, are also depicted. The values of $L_{f\_0.50}$, estimated using the methodology presented above, were used to determine the mean flame height ($L_L$) values required in correlations P2-P4. In all test cases, only estimations of the EVF projection using correlation P1 errs on the safe side, whereas this is not the case for the rest of the correlations.

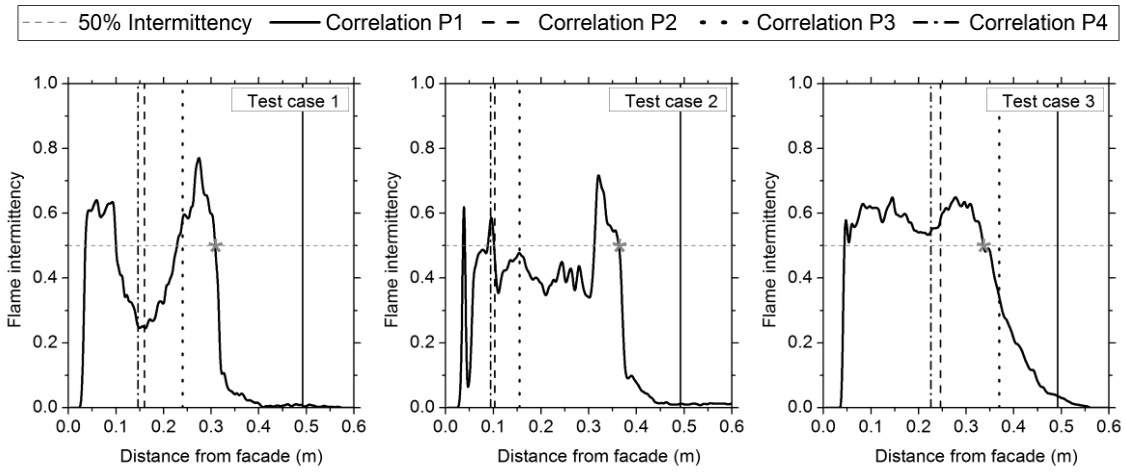


**Figure 9.** Determination of mean flame projection, at a height of 0.9 m, using experimental data and empirical correlations.

In Figure 10, the vertical distribution of the time-averaged EVF width ($w_f$ ) and projection ($L_H$), estimated using the above presented methodology, during the continuous external flaming period, is presented. The EVF width is found to generally increase with increasing height, until it reaches its maximum value, where it starts to decrease again. This remark is not in agreement with the common assumption used in fire design guidelines [6], where $w_f$ remains constant and is considered to be equal to $w_t$ [28]. In Test cases 2 and 3, characterised by relatively larger heat release rate values, a longer EVF projection is generally observed.

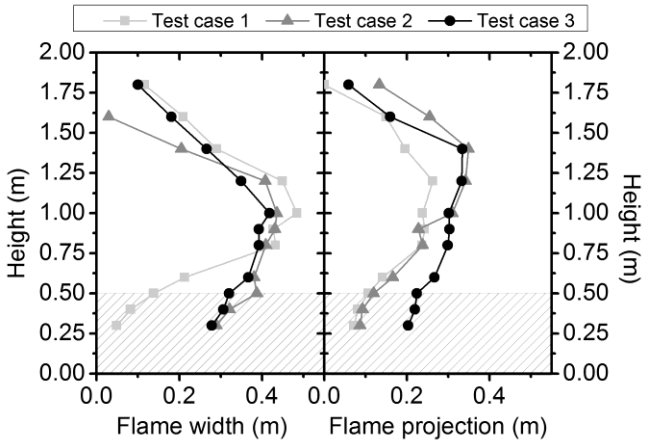


**Figure 10.** Vertical distribution of the time averaged flame width and projection.

## 5. CONCLUSIONS

The objective of this study was the evaluation of available fire engineering design correlations aiming to estimate the geometric characteristics of EVF, using a series of medium-scale compartment-façade fire experiments. Digital camera recordings were used for the determination of the dynamically changing EVF envelope. Predictions using the semi-empirical correlations for the estimation of the EVF height ($L_L$), projection ($L_H$) and width ($w_f$) were compared against the obtained experimental data. Correlations for the estimation of $L_L$ were found to lie on the safe side in under-ventilated fire conditions; increasing the heat release rate results in more conservative predictions for both $L_L$ and $L_H$. Values of flame projection ($L_H$) and flame width ($w_f$) were found to strongly depend on both excess heat release rate from the compartment fire and height from the ground. The necessity to derive appropriate criteria for the identification of $L_H$ was demonstrated.

The obtained extensive set of experimental data, derived for the interior and exterior of the fire compartment, can be used to validate CFD models or evaluate the accuracy of other available fire design correlations. Using medium- and full-scale compartment-façade fire configurations, a range of realistic fire scenarios will be investigated in the future varying a number of established influential parameters such as ventilation conditions, fire load, opening dimensions and relative height of the fuel package. Emphasis will be given in evaluating the accuracy of available semi-empirical correlations and methodologies used for the calculation of EVF envelope, centreline temperatures and heat flux on the façade material.

## 6. ACKNOWLEDGEMENTS

This study has been financially supported by the “Fire-FACTS” project in the frame of the ARISTEIA action (operational programme "Education and Lifelong Learning") that is co-financed by Greece and the E.U. and by the E.C. in the frame of two FP7 projects, "MeeFS: Multifunctional Energy Efficient Façade System for Building Retrofitting" (EeB.NMP.2011-3, Grant No. 285411) and "ELISSA: Energy Efficient Lightweight-Sustainable-Safe-Steel Construction" (EeB.NMP.2013-1, Grant No. 609086). The assistance of Dipl. Eng. Konstantinos Chotzoglou in the development, installation and testing phases of this work is gratefully acknowledged.

## 7. REFERENCES

[1] White N. and Delichatsios M., “Fire Hazards of exterior wall assemblies containing combustible components”, Final Report, Fire Protection Research Foundation, 2014.

[2] Yokoi S., “Study on the prevention of fire spread caused by hot upward current”, Building Research Institute, Report No. 34, Tokyo, Japan, 1960.

[3] Thomas I.R., Moinuddin K.A. and Bennetts I.D., “The effect of quantity and location on small enclosure fires”, *J. Fire Prot. Eng.* 17: 85-102 (2007).

[4] Oleszkiewicz I., “Heat transfer from a window fire plume to a building façade”, Reprinted from “Collected papers in heat transfer”, HTD-Vol. 123, Editors: Marner W.J., Chen T.C., Faghri M., Peterson G.P., Kuehn T.H., Pate M.B., Mahajan R.L. and Lavine A.S., Book No. H00526, 1989.

[5] Tang F., Hu L.H., Delichatsios M.A., Lu K.H. and Zhu W., “Experimental study on flame height and temperature profile of buoyant window spill plume from an under-ventilated compartment fire”, *Int. J. Heat Mass Tran.* 55: 93-101 (2012).

[6] Eurocode 1 (EN 1991-1-2), Actions on structures, Part 1-2 – General Actions – Actions on Structures Exposed to Fire, Brussels, 2002.

[7] Klopovic S. and Turan O.F., “A comprehensive study of externally venting flames, Part I: Experimental plume characteristics for through-draft and no through-draft ventilation conditions and repeatability”, *Fire Safety J.* 36: 99-133 (2001).

[8] Klopovic S. and Turan O.F., "A comprehensive study of externally venting flames, Part II: Plume envelope and center-line temperature comparisons, secondary fires, wind effects and smoke management system", *Fire Safety J.* 36: 135-172 (2001).
[9] Empis C.A., "Analysis of the compartment fire parameters influencing the heat flux incident on the structural façade", PhD University of Edinburg, 2010.
[10] Himoto K., Tsuchihashi T., Tanaka Y. and Tanaka T., "Modeling thermal behaviors of window flames ejected from a fire compartment", F*ire Safety J.* 44: 230-240 (2009).
[11] Asimakopoulou E., Kolaitis D. and Founti M., "Comparative assessment of CFD tools and the Eurocode methodology in describing Externally Venting Flames", 1st International Seminar for Fire Safety of Façades, 14-15 November 2013, Paris, France.
[12] Heskestad G., "Virtual origins of fire plumes", *Fire Safety J.* 5:109-114 (1983).
[13] Law M., "Fire safety of external building elements – The design approach", *AISC Engineering Journal*, Second Quarter, 1978.
[14] Beyler C.L., "Fire plumes and ceiling jets", *Fire Safety J.* 11:53-75 (1986).
[15] Hasemi Y. and Tokunaga T., "Flame geometry effects in the buoyant plumes from turbulent diffusion flames", *Fire Safety Science and Technology* 4:15-26 (1984).
[16] McCaffrey B.J., "Momentum implications for buoyant diffusion flames", *Combust. Flame* 52:149-156 (1983).
[17] Beuther P.D. and George W.K., "Measurement of the turbulent energy and temperature balances in an axisymmetric buoyant plume in a stably stratified environment", *Proc. of the 7th Int. Heat Trans. Conf.*, 163-178, Munich 1982, Hemisphere Press, NY.
[18] Delichatsios M., Lee Y., Tofilo P., "A new correlation for gas temperature inside a burning enclosure", *Fire Safety J.* 44:1003-1009 (2009).
[19] Korhonen T. and Hietaniemi J., "Fire safety of wooden façades in residential suburb multi-storey buildings", VTT Working Papers 32, July 2005.
[20] ISO 9705, International Organization for Standardization: Geneva, Switzerland, ISO 9705, "Fire Tests: Full-Scale Room Test for Surface Products", First Edition, 1993.
[21] Vipin V., "Image processing based forest detection", *International Journal of Emerging Technology and Advanced Engineering* 2:87-95 (2012).
[22] Celik T., Demirel H., Ozkaramanli H. and Uyguroglu M., "Fire detection using statistical color model in video sequences", *J. Vis. Commun. Image R.* 18:176-185 (2007).
[23] Audoin L., Kolb G., Torero J.L. and Most J.M., "Average centreline temperatures of a buoyant pool fire obtained by image processing of video recordings", *Fire Safety J.* 24:167-187, 1995.
[24] DiNenno P.J., Drysdale D., Beyler C.L., Walton W.D., Custer R.L.P., Hall J.R. and Watts J.M.,"SFPE Handbook of fire protection engineering", Tien C.L., Lee K.Y. and Stretton A.J., Chapter 4 "Radiation Heat Transfer", Third Edition, SFPE, Quincy, Massachusetts, 2002.
[25] Thomas P.H. and Law M., "The projection of flames from burning buildings", Fire Research Station, Fire Research Note, No 921, Borehamwood, USA, 1972.
[26] Hu L., Lu K., Delichatsios M., He L. and Tang F., "An experimental investigation and statistical characterization of intermittent flame ejecting behaviour of enclosure fires with an opening", *Combust. Flame* 159:1178-1184 (2012).
[27] Gottuk D.T., Roby R.J. and Beyler C.L., "A study of CO and smoke yields from compartment fires with external burning", *Proc. Comb. Inst.* 24:1729-1735 (1992).
[28] Lee Y., Delichatsios M.A. and Silcock G.W.H., "Heat flux distribution and flame shapes on the inert façade", *Fire Safety Science* 9:193-204 (2008).